

See discussions, stats, and author profiles for this publication at: <https://www.researchgate.net/publication/258501191>

# Theoretical Modeling of Deuteration-Induced Shifts of the o-o Bands in Absorption Spectra of Selected Aromatic Amines: The Role of the Double-Well Potential

ARTICLE *in* THE JOURNAL OF PHYSICAL CHEMISTRY A · NOVEMBER 2013

Impact Factor: 2.69 · DOI: 10.1021/jp407987y · Source: PubMed

---

CITATIONS

3

---

READS

18

## 2 AUTHORS:



**Marcin Andrzejak**

Jagiellonian University

38 PUBLICATIONS 360 CITATIONS

SEE PROFILE



**Przemysław Kolek**

Rzeszów University

21 PUBLICATIONS 146 CITATIONS

SEE PROFILE

# Theoretical Modeling of Deuteration-Induced Shifts of the 0–0 Bands in Absorption Spectra of Selected Aromatic Amines: The Role of the Double-Well Potential

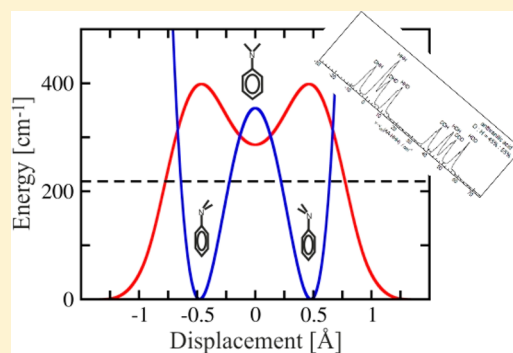
Marcin Andrzejak<sup>†,\*</sup> and Przemysław Kolek<sup>‡</sup>

<sup>†</sup>K. Gumiński Department of Theoretical Chemistry, Faculty of Chemistry, Jagiellonian University, Kraków, 30-060, Poland

<sup>‡</sup>Atomic and Molecular Physics Laboratory, Institut of Physics, University of Rzeszów, Rzeszow, 35-959, Poland

## S Supporting Information

**ABSTRACT:** The harmonic approximation fails for inversion of the NH<sub>2</sub> group in the ground state of aromatic amines as this vibration is characterized by a symmetric double-well potential with relatively small energy barrier. In such cases, the standard harmonic vibrational analysis is inapplicable: the inversion frequency calculated for the bottom of the potential well is strongly overestimated, while it attains imaginary values for the planar conformation of the molecule. The model calculations are discussed taking explicitly into account the presence of the double-well potential. The study is initially focused on reproduction of the deuteration-induced shifts of the 0–0 absorption band for anthranilic acid. The (incorrect) harmonic frequency of the NH<sub>2</sub> inversion is replaced by a better one, obtained from numerical calculations employing a simple, quartic-quadratic model for the double-well potential, which is parametrized using just the harmonic frequency of the inversion and the height of the energy barrier. This operation brings theoretical results to qualitative agreement with experiment. A still better match is achieved with a modified version of the model that accounts for mixing of the NH<sub>2</sub> inversion mode with other normal modes while retaining the initial simplicity of one-dimensional approach. The corrected results show surprisingly good accuracy, with deviations of the calculated shifts from the experimental values reduced to less than 5 cm<sup>−1</sup>. In order to test the performance of the model for systems with higher energy barrier for the NH<sub>2</sub> inversion, we have measured the LIF excitation spectra of three different aminobenzonitriles. Partial assignment of the 0–0 bands has been achieved based on their relative intensities for samples with different isotopic exchange ratios. Calculated shifts are in excellent agreement with experimental values for the identified bands. Theoretical predictions are used to complete the assignment of the 0–0 bands in the spectra of the studied aminobenzonitriles.



## I. INTRODUCTION

Aromatic compounds containing the NH<sub>2</sub> group have been widely studied both experimentally and theoretically.<sup>1–8</sup> The organic chromophore provides the oscillator strength, whereas the amino group is the source of nontrivial vibronic effects. The nitrogen atom in aliphatic amines is sp<sup>3</sup>-hybridized, and the amino group assumes the pyramidal conformation. In aromatic amines the aromatic system is usually planar, and the inversion of the amino group flips the system between two minima corresponding to the pyramidal conformations of the NH<sub>2</sub> group. The height of the energy barrier for inversion strongly depends on the coupling of the lone electron pair of the nitrogen atom with the delocalized  $\pi$ -electron system of the aromatic part of the molecule.<sup>9</sup> If the coupling is strong, it lowers the energy barrier and induces partial or even complete planarization of the amino group. Thus, by a careful choice of the substituents it is possible to control the energy barrier for inversion. In the excited state, owing to the rearrangement in the  $\pi$ -electron system, the amino group usually becomes planar

(or nearly so), with the nitrogen atom adopting the (approximately) sp<sup>2</sup> hybridization.

In the case of a high energy barrier, the molecule in the ground state basically resides in one of the energy basins corresponding to the pyramidal conformations of the NH<sub>2</sub> group, with a small probability of tunneling through the barrier. Standard vibrational analysis performed for such a nonplanar ground state geometry can usually reach reasonable agreement with experimental data (the small tunneling splitting of the vibrational energy levels, neglected in such a simple approach, is often experimentally undetectable). When the energy barrier is low, vibronic structures in the optical spectra (UV/vis absorption or fluorescence) can be rationalized theoretically assuming planar conformations for both the ground and the excited state of the molecule. The NH<sub>2</sub> inversion has to be excluded from vibrational analysis for the planar ground state,

Received: August 9, 2013

Revised: November 8, 2013

Published: November 12, 2013

as it acquires imaginary frequency at the top of the energy barrier. The coupling of the higher frequency in-plane vibrations with the inversion is usually rather weak, therefore inappropriate treatment of this normal mode does not significantly affect the reproduction of vibronic structures observed in the experimental spectra.<sup>8,10,11</sup> This approach can be better understood by regarding the low energy barrier for inversion as a small perturbation to the otherwise mostly harmonic potential. The vibrational wave functions for this normal mode resemble the solutions for the harmonic oscillator. In particular, the maximum of the ground state vibrational wave function corresponds to the planar conformation of the NH<sub>2</sub> group, being just slightly wider than for the parent harmonic solution (cf. figures in section 7). The molecule can thus be described as dynamically planar, even though the equilibrium geometry is distorted from planarity. When the energy barrier gets higher, the picture outlined above becomes increasingly more complicated, and the correspondence between the harmonic wave functions and the exact solutions becomes less evident. The probability of the molecule assuming the approximately planar conformation no longer dominates, even though the likelihood of switching from one distorted conformation to the other (NH<sub>2</sub> inversion) is still high. In such a case, no single conformation can describe the ground state geometry of the molecule, and the vibrational solutions for the amino group inversion have to be obtained numerically once the double-well potential has been modeled with a sufficient accuracy. Fortunately, in many cases the coupling between the inversion and the in plane vibrations may still be weak, and the most important vibronic features of the spectra (often corresponding to the in-plane vibrations) may be reproduced with good accuracy based on vibrational analysis for the planar conformation in the ground electronic state.<sup>8</sup>

Some experimental results, however, cannot be correctly reproduced even in the limiting cases of the small energy barrier. An example of such a situation are the relative positions of the 0–0 bands for various deuteromers in the absorption spectra of the anthranilic (*p*-aminobenzoic) acid (AA). AA contains three easily interchangeable hydrogen atoms (see Figure 1) that can be replaced by deuterium through reaction with heavy water D<sub>2</sub>O.

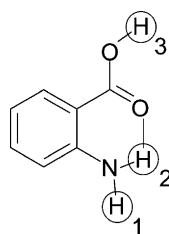


**Figure 1.** The schematic representation of the AA molecule, showing the interchangeable hydrogen atoms.

Unfortunately, this process usually leads to a mixture of isotopomers, their relative concentrations depending on the D<sub>2</sub>O/H<sub>2</sub>O ratio. Moreover, in the supersonic jet experiments, even an initially pure, fully deuterated species (DDD-AA) undergoes a reverse substitution reacting with traces of water present in the experimental setup.<sup>12</sup> In such a situation, analysis of the highly resolved vibronic spectra from the SS-Jet measurements becomes a formidable task, as they consist of the complex overlapping structures corresponding to various

isotopomers. An independent way to estimate the relative positions of the electronic origins of the spectra for different isotopomers would certainly aid the analysis of the experimental results. Nowadays, one usually resorts to quantum chemistry (usually DFT) calculations to access the molecular properties for both the ground state and the electronic excited states. The energy of the 0–0 band of the vibronic structure in the absorption spectrum consists of the adiabatic excitation energy from the equilibrium geometry of the ground state to a given electronic state (taken after geometry relaxation) and the difference between the zero point energies (ZPE) for both states:

$$E_{0-0} = E_{\text{exc}}^a + (\text{ZPE}_{\text{exc}} - \text{ZPE}_{\text{gr}}) \quad (1)$$

Within the Born–Oppenheimer (BO) approximation, isotopic substitution does not change the electronic excitation energy, affecting only the vibrational frequencies, and through them the ZPEs. Therefore, if one uses the standard quantum chemistry calculations (based on the BO approximation), the relative positions of the 0–0 bands for different isotopomers depend only on the changes of the  $\Delta\text{ZPE} = \text{ZPE}_{\text{exc}} - \text{ZPE}_{\text{gr}}$  due to the isotopic substitution.

For the AA, however, this simple (albeit approximate) picture is not suitable, owing to the presence of the double-well potential for the NH<sub>2</sub> inversion in the ground electronic state that changes to the approximately harmonic potential upon the S<sub>0</sub> → S<sub>1</sub> electronic excitation. Low energy barrier for inversion in the ground state makes the molecule dynamically planar, but from the point of view of the standard quantum chemistry calculations, the planar conformation corresponds to the maximum on the potential energy surface (PES). The frequency of inversion is thus imaginary and cannot be included in the ZPE<sub>gr</sub>. In the excited state, the equilibrium geometry of the molecule is planar, therefore all vibrations contribute to the ZPE<sub>exc</sub>. The  $\Delta\text{ZPE}$  is therefore *overestimated* when the planar conformation is assumed for the ground state. There is, however, another possibility: one may choose the nonplanar conformation for the electronic ground state, corresponding to one of the minima on the PES for inversion of the amino group. Since it is a genuine minimum, all the normal modes have real frequencies and are included in the ZPE<sub>gr</sub>. Unfortunately, the curvature in the vicinity of the minimum is bound to be overestimated, since two minima of the double-well potential have to find room in the energy basin, which in the hypothetical case of the unperturbed PES (no barrier) would need to accommodate only one minimum (corresponding to the planar conformation). Consequently, the ZPE<sub>gr</sub> will be overshoot, leading to the *underestimated* value of the  $\Delta\text{ZPE}$ . Evidently, accurate reproduction of the  $\Delta\text{ZPE}$  cannot be obtained through the harmonic analysis at either of the stationary points on the ground state PES for the NH<sub>2</sub> inversion. Moreover, the errors will not be the same for different isotopomers. The amino group contains two of the three interchangeable hydrogen atoms, so the isotopic exchange obviously changes the frequency of inversion, and by that also the ZPEs. Consequently, the errors are dependent on the degree of deuteration. For AA the situation is further complicated by the fact that one of the hydrogen atoms of the NH<sub>2</sub> group is involved in the formation of the intramolecular hydrogen bond (the bridge atom) with the carbonyl oxygen atom of the COOH group. The hydrogen atoms of the amino group are thus not equivalent, and the hydrogen atom of the carboxylic group (the third interchange-

able atom) has an additional connection with them through the hydrogen bond. As a result, it is rather difficult to predict *a priori* the influence of deuteration on the positions of the origin bands in the absorption spectrum of AA.

In order to achieve correct theoretical reproduction of the relative positions of the 0–0 bands for different deuteromers of AA, one has to consider going beyond the harmonic approximation. Ideally, a multidimensional potential should be constructed that would include both large-amplitude low-frequency out-of-plane vibrations of the amino group (inversion and torsion) together with the few small-amplitude normal modes that are coupled to the former two (e.g., C–N stretching and NH<sub>2</sub> bending).<sup>13,14</sup> For aniline, such an approach gave very accurate reproduction of the frequencies for the fundamental vibrational levels of both the NH<sub>2</sub> inversion and torsion, their overtones, and the combination bands.<sup>9</sup> It would require, however, a considerable computational effort to parametrize the multidimensional potential energy surface for AA, especially in view of the C<sub>1</sub> symmetry of the system. In a less rigorous approach the coupling of the NH<sub>2</sub> inversion with all the other normal modes can be neglected, so that the inversion is modeled in one dimension. Even though it is a serious simplification, such an approach was successfully applied to reproduce the experimental frequencies of the fundamental band and the first overtone of the out-of-plane NH<sub>2</sub> vibration of 2-aminopyrimidine.<sup>15</sup> In this work we also use an essentially one-dimensional approach to the NH<sub>2</sub> inversion of AA, but the anharmonic potential for the inversion is modeled by the quartic-quadratic function—a natural expansion of the harmonic potential obtained by including the next nonvanishing term of the Taylor expansion of the actual potential energy function. The important advantage of the quartic-quadratic function is that it can be parametrized using the results of the standard quantum chemistry results—the harmonic frequencies calculated at the bottom of the potential well and the height of the energy barrier. We examine to what extent such a rectification of the fundamentally incorrect harmonic potential improves the theoretical results, discuss the possible sources of errors, and eventually extend our model to account for coupling of the NH<sub>2</sub> inversion with other normal modes, while retaining its essential simplicity. Eventually, in order to test the performance of both models in more challenging cases of intermediate energy barriers, we report and analyze the experimental spectra of three different amino-bezonitriles, recorded for samples with varying levels of deuteration. Origin bands for the pristine and completely deuterated species have been identified based on the experimental line intensities, and, by comparing their position with theoretical results, we could test the performance of the proposed models. Then the calculated shifts have been used to identify the yet unassigned origin bands.

## 2. COMPUTATIONAL DETAILS

Nowadays, the first choice of methodology applicable for a system like the AA would be DFT, probably using a hyper-GGA exchange-correlation (XC) functional with moderate content of nonlocal exchange (e.g., B3LYP,<sup>16–18</sup> or PBE0<sup>19</sup>). Current implementations of DFT (and TDDFT for the excited states) usually allow for geometry optimizations using analytical gradients and vibrational analysis with analytical Hessians for both the ground and the electronic excited states. Since the S<sub>1</sub> excited state of AA is dominated by the singly excited electronic configurations (mostly the HOMO→LUMO one), the

accuracy of DFT should be quite good. Unfortunately, our preliminary DFT calculations (performed with a number of XC functionals) showed that DFT wrongly predicts the planar conformation as the optimum structure for the ground state of AA. The choice of alternative methods that allow for geometry optimization and vibrational analysis not only for the ground electronic state, but also for the excited state is limited. For the purpose of this study we have selected the CC2 method—the approximate version of CCSD, in which double excitations are introduced perturbatively (analogously to MP2), whereas single excitations are fully included, which allows for relaxation of orbitals and thus for modeling the molecular response to external perturbation.<sup>20,21</sup> The CC2 calculations are much less computationally demanding than the parent CCSD ones, and they are surprisingly accurate for molecular geometries and harmonic frequencies,<sup>22,23</sup> as well as excitation energies,<sup>24</sup> provided the wave function of the excited state does not contain large contributions of doubly excited configurations. Current implementation (Turbomole 6.3) has analytical gradients for geometry optimization in both the ground<sup>22</sup> and the excited state.<sup>23</sup> Unfortunately, the Hessian required for the vibrational analysis still has to be calculated numerically, which is computationally demanding and prevents going beyond the harmonic approximation. All our calculations using CC2 were carried out with the Turbomole 6.3 package of programs.<sup>25</sup> We have also used the Turbomole implementations of MP2, CCSD, and CCSD(T), as well as their explicitly correlated versions<sup>26–28</sup> in order to estimate the energy barrier for inversion of the amino group in AA.

## 3. THE MODEL

Before describing the model used to correct the shifts of the 0–0 bands based on the standard quantum chemistry calculations, we present the uncorrected results to show the deficiencies of using either of the stationary points on the PES for inversion of the NH<sub>2</sub> group (the minima or the maximum of the energy barrier). Figure 2 shows the plot of the calculated and the experimental shifts of the 0–0 lines in the absorption spectra of all eight deuteromers of AA. The experimental shifts of the 0–0 bands display interesting regularities. The largest effect (43–44 cm<sup>–1</sup>) follows substitution of the bridge hydrogen atom (site 2), which is involved in formation of the intramolecular

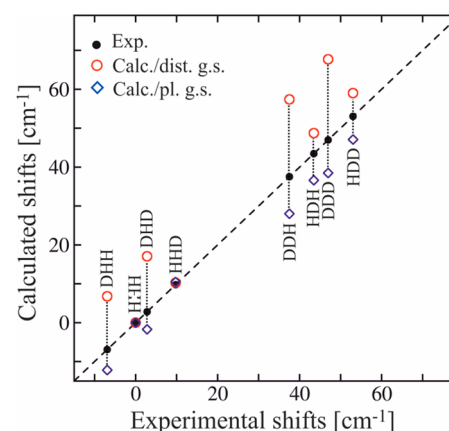


**Figure 2.** Uncorrected shifts of the 0–0 bands for all deuteromers of AA calculated (CC2/aug-cc-pVDZ) at the minimum of the double-well potential (red circles) and at the top of the energy barrier (blue diamonds) with respect to the experimental values (black dots).



hydrogen bond. Deuteration of the other site on the amino group (site 1) results in the red shift of 6–7 cm<sup>-1</sup>. Deuteration at site 3 (carboxyl group) brings about a blue shift of 10 cm<sup>-1</sup>. The shifts seem to be quite independent of one another.

The calculated values of the shifts, obtained through the harmonic vibrational analysis agree with the experimental ones only for the HHD isotopomer, which indicates that the site at the carboxylic group is practically decoupled from the NH<sub>2</sub> inversion. Relatively small errors are also observed for the HDH and HDD species. The most striking are the discrepancies for the isotopomers deuterated at site 1. The errors are such that they change the ordering of the calculated positions of the 0–0 bands with respect to experiment. Interestingly, if the calculations are carried out for the nonplanar ground-state conformation of AA, the errors are positive, whereas for the planar conformation, they are negative with respect to the experimental results. The signs of the errors are thus in accord with our expectations (vide supra).

In attempt to correct the results based on the harmonic vibrational analysis for the distorted conformation of AA we replace the overshoot frequencies of the NH<sub>2</sub> inversion (obtained for the distorted conformation) with the frequencies calculated using a one-dimensional model of the double well potential. All the other normal modes are initially assumed to be unaffected by this operation. This assumption is not entirely satisfied, as the inversion of the amino group is strongly coupled with the NH<sub>2</sub> torsion, and to some extent also with the NH<sub>2</sub> bending as well as the CN stretching.<sup>9</sup> This coupling is the potential source of errors of the one-dimensional approach and it is further approximately accounted for in the quasi-multimode version of the model. The double well potential for inversion of the NH<sub>2</sub> group is represented by the quartic-quadratic function, obtained in a natural way by adding to the harmonic potential the next nonvanishing term in the Taylor expansion of the potential energy:

$$V(q) = aq^4 - bq^2 + \frac{b^2}{4a} \quad (2)$$

The quartic-quadratic function is known to fit accurately the vibrational levels of the symmetric double minima.<sup>29–31</sup> It is also easily parametrized by the harmonic frequency of the NH<sub>2</sub> inversion  $\tilde{\nu}$  at the minimum, and by the barrier height  $\Delta$ :

$$b = \frac{1}{2}\pi^2\mu\tilde{\nu}^2, \quad a = \frac{b^2}{4\Delta} \quad (3)$$

$\mu$  is the reduced mass for the inversion, easily available through the vibrational analysis for the planar AA, for which the relevant normal mode is marked by its imaginary frequency. Rigorously, for the quartic-quadratic potential the ratio of the frequencies for the minimum and for the top of the energy barrier would be  $\tilde{\nu}_{C_1}/|\tilde{\nu}_{C_2}| = \sqrt{2}$ . The real ground-state potential, however, is neither strictly quartic-quadratic, nor does it follow the direction of a single normal mode – at the bottom of the potential well the inversion becomes mixed with other vibrations (e.g., the torsion of the amino group). Moreover, the constitution of the normal coordinates depends on which hydrogens are replaced by deuterium atoms. It is thus by no means trivial to select a single mode for the model calculations. Initially, for every isotopomer the vibration closest to the NH<sub>2</sub> inversion was selected by choosing the normal mode that was characterized by large, out-of-plane, and in-phase motions of the two hydrogen atoms of the amino group. This choice was

further corroborated by the vibrational frequency being approximately  $\sqrt{2}$  times larger than the modulus of the imaginary frequency calculated for the respective planar conformer. Having performed the PED analysis (as implemented in Turbomole 6.3), however, we observed that sizable contents (brutto) of the NH<sub>2</sub> inversion could be found not only in the previously selected vibrations, but also in a number of other normal modes of similar frequencies. Therefore, we modified our approach in such a way that would allow us to include all the inversion containing normal modes, retaining the simple one-dimensional quartic-quadratic potential. To do that, we parametrized the potential for each of the above-mentioned normal modes of a given isotopomer, using their respective frequencies. The total correction to the ground state ZPE was then obtained as the sum of the individually calculated corrections for all the above-mentioned vibrations weighted by the contents brutto ( $w_i$ ) of the NH<sub>2</sub> inversion (obtained in the PED analysis):

$$\text{ZPE}_{\text{gr}}^{\text{corr.}} = \text{ZPE}_{\text{gr}} + \frac{1}{2} \sum_i w_i (v_i^{\text{model}} - v_i^{\text{q.chem}}) \quad (4)$$

Such a quasi-multimode, or “weighted”, approach is a consequence of using the one-dimensional model for the inherently multidimensional case. Alternatively, one could construct and parametrize a truly multimode model including all the vibrations coupled with the inversion of the NH<sub>2</sub> group. It would, however, require a tremendous conceptual and computational effort, while its benefits could be obscured by errors arising from standard approximations of the quantum chemistry calculations, e.g., the errors of the harmonic approximation used for all the normal modes not involved in the motion of the NH<sub>2</sub> group. It is therefore prudent to venture first a relatively simple approach to assess what is the impact the quartic correction to the harmonic potential for the NH<sub>2</sub> inversion on theoretical reproduction of the experimental data, and to determine how seriously other approximations influence the accuracy of theoretical results. Based on these observations, rational modifications to the one-dimensional approach may be designed in order to improve its accuracy.

#### 4. THE ENERGY BARRIER FOR INVERSION

The energy barrier for inversion of the amino group is one of the two quantities that parametrize the model in our study. To estimate its value we have selected several ab initio methods using the approximate N-electron wave function of increasing quality: MP2, CC2, CCSD, and CCSD(T) in combinations with the Dunning correlation consistent basis sets:<sup>32</sup> cc-pVXZ with X = D, T, Q, 5, 6, and aug-cc-pVXZ, with X = D, T, Q, 5. The correlation consistent basis sets are constructed in such a way that they allow for extrapolation of the results to the complete basis set (CBS) limit.<sup>33</sup> The energy barrier has been calculated as difference of the ground-state electronic energy of AA for the planar conformation, and for the distorted one. The results have been obtained for geometries optimized with the aug-cc-pVDZ basis set. They are displayed in Figure 3, and collected in Table 1. The results of the MP2 (and CC2) calculations show that the dependence of the calculated energy barrier on the basis set size is much weaker for the aug-cc-pVXZ series of basis sets than for the cc-pVXZ one. It shows that the diffuse functions are very important for modeling of the energy barrier, and potentially for other inversion-related properties of AA. Note, however, that the decreasing trend of the energy barrier

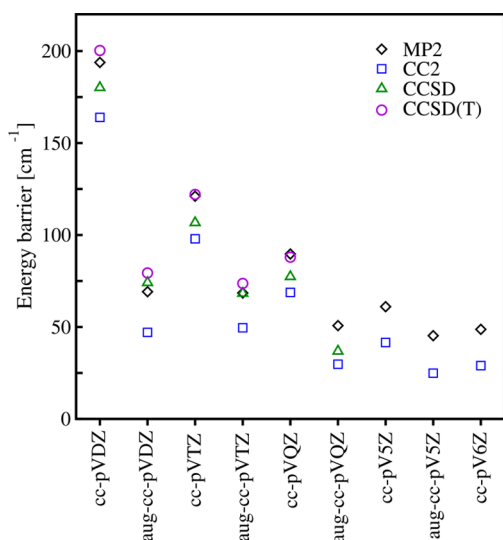


**Figure 3.** Energy barrier for inversion, as calculated with the selected ab initio methods and a sequence of correlation-consistent basis sets.

with the basis set cardinal number ( $X$ ) is not smooth—the aug-cc-pVTZ result is almost as high as the aug-cc-pVDZ one, and noticeably higher than the values obtained with the two largest augmented basis sets (cf. Table 1). Nonetheless, the energy barrier extrapolated from the results obtained with the two largest basis sets in both series (cc-pV5Z/cc-pV6Z, and aug-cc-pVQZ/aug-cc-pV5Z) are within the margin of  $3 \text{ cm}^{-1}$  from one another, which indicates that these values are already close to the genuine CBS limit for the MP2 calculations.

The results for the CC2 method, apart from being uniformly shifted to lower energies by about  $20 \text{ cm}^{-1}$ , behave analogously to the MP2 results. The CCSD calculations yield values for the energy barrier comparable to the MP2 results (slightly above the MP2 values for the augmented basis sets), while inclusion of triply excited configurations in the CCSD(T) method shifts the calculated energy barriers up by  $5\text{--}10 \text{ cm}^{-1}$  for the larger basis sets. Unfortunately, for the CCSD or CCSD(T) calculations scale unfavorably with the number of orbitals ( $N^6$  and  $N^7$ , respectively) and we were unable to carry out the calculations for the largest basis sets ( $n \geq 5$ ) that would allow for accurate CBS extrapolations. Judging from the relations between the MP2, CCSD and CCSD(T) results computed with the same basis sets, however, one can assume that the  $E_{\text{CBS}}^{\text{CCSD(T)}}$  value should be close to (or slightly higher than)  $40 \text{ cm}^{-1}$ , the value based on the most accurate MP2 extrapolations.

In view of the strong basis set dependence of the energy barrier, we have carried out additional calculations employing the explicitly correlated versions of the MP2, CCSD, and CCSD(T) calculations. The explicitly correlated methods are characterized by rapid convergence of the correlation energy toward the CBS limit.<sup>27</sup> The deviations are proportional to  $(L + 1)^{-7}$ ,  $L$  being the largest angular momentum quantum number represented in the orbital basis. The MP2-F12 values of the energy barrier obtained with the optimized cc-pVXZ-F12 basis sets ( $X = \text{D, T, Q}$ ) are  $51.5 \text{ cm}^{-1}$ ,  $49.0 \text{ cm}^{-1}$ , and  $44.3 \text{ cm}^{-1}$ , respectively. Analogous values from the CCSD(F12) method ( $X = \text{D, T}$ ) are very similar:  $51.7 \text{ cm}^{-1}$  and  $45.4 \text{ cm}^{-1}$ , while CCSD(T)(F12)/cc-pVDZ calculations yield the value of  $64.9 \text{ cm}^{-1}$ . Thus obtained energy barriers are consistent with the best CBS-extrapolated values from the conventional calculations.

In view of the above results, one may safely conclude that the energy barrier for inversion in AA is very low, probably between  $40$  and  $55 \text{ cm}^{-1}$ , which is in accordance with the observations that AA is dynamically planar in the ground state.<sup>12,34</sup> Moreover, it seems that using the energy barrier obtained at the CC2/aug-cc-pVXZ ( $X = \text{D, T}$ ) or CC2/cc-pVQZ levels of theory, instead of the explicitly correlated results or the CBS-extrapolated values, would not introduce significant errors into the model calculations (for details of the energy barrier influence on the results of the model calculations, the reader is referred to the Supporting Information). On the other hand, it would have the advantage of consistency—the geometries, vibrational analyses for both the ground and the excited state, and the energy barrier would be obtained with the same method and basis set.

## 5. VIBRATIONAL ANALYSIS

Geometries of the AA have been optimized at the CC2 level of theory for both the planar and the distorted ground-state conformations of the molecule, as well as for the planar conformation in the lowest excited state. We used three basis sets: aug-cc-pVDZ, aug-cc-pVTZ, and cc-pVQZ, for which the height of the energy barrier is close to the CBS limit. For each of the stationary points (the minimum and the top of the barrier), we have obtained harmonic frequencies and normal coordinates. The accuracy of the vibrational frequencies can be checked against the experimental data for the HHH-AA for both the ground state and the lowest excited state. The experimental and the calculated frequencies are collected in Table 2. We have considered only the high frequency stretches of hydrogen atoms because the experimental data are complete

**Table 1.** Energy Barriers (in  $\text{cm}^{-1}$ ) Obtained with Different Ab Initio Methods and Correlation-Consistent Basis Sets<sup>a</sup>

	$n$	MP2	CC2	CCSD	CCSD(T)
cc-pVXZ	D	193.8	164.0	180.2	200.3
	T	121.1 (113.7)	97.9 (94.0)	108.7 (99.0)	122.1 (113.7)
	Q	89.7 (77.1)	68.8 (57.9)	77.4 (66.3)	87.9 (73.4)
	5	61.0 (43.6)	41.6 (25.6)		
	6	48.7 (37.9)	29.0 (17.8)		
aug-cc-pVXZ	D	69.2	47.1	74.1	79.4
	T	68.5 (62.8)	49.3 (58.7)	68.3 (75.8)	73.7 (79.3)
	Q	50.7 (38.6)	29.8 (18.2)		
	5	45.3 (40.1)	24.9 (20.3)		

<sup>a</sup>Numbers in parentheses represent the energies extrapolated to the CBS limit<sup>33</sup> from the results obtained using two basis sets with the respective cardinal numbers equal to  $X$  and  $X - 1$ .

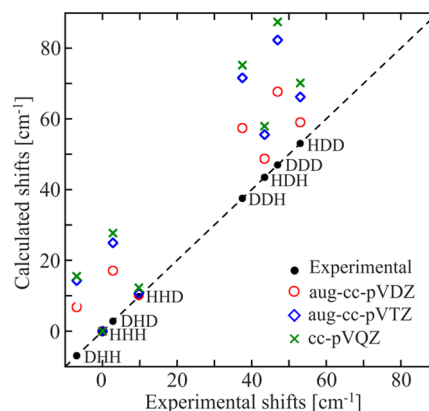
**Table 2.** Experimental and Calculated Frequencies for the Ground State (in the Planar and Distorted Conformations) and for the Excited State

		planar conformation			distorted conformation			exp. <sup>a</sup>
		aug-DZ	aug-TZ	QZ	aug-DZ	aug-TZ	QZ	
ground State	$\nu_{\text{OH}}$	3686	3695	3720	3686	3698	3724	3592
	$\nu_{\text{NH}}^{\text{a}}$	3717	3720	3737	3672	3681	3694	3542
	$\nu_{\text{NH}}^{\text{s}}$	3531	3536	3550	3501	3509	3521	3394
	$\nu_{\text{CH}}$	3237	3231	3240	3237	3231	3240	3093
	$\nu_{\text{CH}}$	3221	3215	3225	3221	3215	3225	3073
	$\nu_{\text{CH}}$	3205	3200	3207	3205	3199	3208	3063
	$\nu_{\text{CH}}$	3185	3179	3188	3184	3179	3189	3038
	$\nu_{\text{C=O}}$	1671	1681	1693	1674	1686	1718	1728
excited State	$\nu_{\text{OH}}$	3700	3712	3732				3604
	$\nu_{\text{NH}}^{\text{a}}$	3597	3602	3617				3460
	$\nu_{\text{NH}}^{\text{s}}$	2910	2888	2896				2900
	$\nu_{\text{CH}}$	3242	3233	3241				3095
	$\nu_{\text{CH}}$	3236	3225	3235				3095
	$\nu_{\text{CH}}$	3205	3195	3204				3060
	$\nu_{\text{CH}}$	3191	3181	3190				3045
	$\nu_{\text{C=O}}$	1677	1678	1686				1650
Frequency Differences $\Delta(\text{exc-gr})$ between the Excited and the Ground State								
	$\nu_{\text{CH}}^{\text{a}} \nu_{\text{OH}}$	40	26	22	41	24	16	40
	$\nu_{\text{NH}}^{\text{a}} \nu_{\text{NH}}^{\text{s}} \nu_{\text{C=O}}$	-735	-769	-781	-663	-708	-734	-654
	total	-695	-743	-759	-622	-684	-718	-614
$\Delta(\text{exc-gr})_{\text{experimental}} - \Delta(\text{exc-gr})_{\text{calculated}}$								
	$\nu_{\text{CH}}^{\text{a}} \nu_{\text{OH}}$	0	14	18	-1	16	24	
	$\nu_{\text{NH}}^{\text{a}} \nu_{\text{NH}}^{\text{s}} \nu_{\text{C=O}}$	81	115	127	9	54	80	
	total	81	129	145	8	70	104	

<sup>a</sup>All the experimental data from ref.<sup>35</sup> except for the C=O stretch for the ground state<sup>36</sup> and for the excited state<sup>37</sup>

for this spectral region, and the C=O stretching mode since the C=O group is involved in the intramolecular hydrogen bond. The high frequency vibrations give the largest contributions to the ZPEs and therefore their correct reproduction is essential for analyzing the deuteration-induced shifts of the 0–0 bands. Moreover, the N–H stretches undergo very large frequency changes upon deuteration, which are bound to have strong impact on the shifts of the 0–0 bands.

The harmonic frequencies are grossly overestimated with respect to the experimental values. The differences between the excited state and the ground state ( $\Delta(\text{exc-gr})$ ), however, compare much more favorably with experiment. The agreement is especially good for the aug-cc-pVDZ results. The difference for the C–H and the O–H stretches is reproduced perfectly, regardless of the ground-state conformation adopted in the calculations. For the N–H and the C=O stretches, however,  $\Delta(\text{exc-gr})$  is significantly affected by the choice of the ground-state conformation. It was only to be expected, as the nitrogen atom is the center of all the conformational differences, and the C=O group is linked with the amino group by the internal hydrogen bond. Again, the agreement with experiment is the best for the aug-cc-pVDZ results, but in this case the error is small only for the nonplanar ground state geometry (8 cm<sup>-1</sup>), whereas for the planar one the calculated frequency difference is considerably overshoot (81 cm<sup>-1</sup>). The best performance of the aug-cc-pVDZ basis set can also be observed for the calculated relative shifts of the 0–0 lines for various isotopomers of AA. They are presented in Figure 4. The errors for the aug-cc-pVTZ, and especially for the cc-pVQZ basis sets are nearly twice as large as the errors for the aug-cc-pVDZ one. Although it seems at first somewhat counter-intuitive that the discrepancies of  $\Delta(\text{exc-gr})$  with respect to the

**Figure 4.** Calculated (assuming the nonplanar ground state conformation) versus experimental shifts of the 0–0 bands of isotopomers of AA, obtained with three different basis sets.

experimental values are the smallest for the relatively modest aug-cc-pVDZ basis set, one has to bear in mind that we are comparing the vibrational frequencies calculated at the harmonic level with the experimental ones, which are by no means harmonic. Therefore in principle there is no reason to expect systematic reduction of errors in calculated frequencies for larger basis sets. Besides, the quantum chemistry methods themselves need not necessarily give improved results upon enlargement of the basis set (apart from the energy of the system for variational methods), as the accuracy depends also on the choice of approximate model for the N-electronic wave function.<sup>38,39</sup>

**Table 3. Selected Normal Modes for Different Isotopomers of the AA, the Contributions of the NH<sub>2</sub> Inversion (%inv), and the Respective Parameters for the Model Potential**

HHH $ \tilde{\nu}_{C_1}  = 217.7 \text{ cm}^{-1} \mu_{Cs} = 1.47$	$\tilde{\nu}_{C_1} [\text{cm}^{-1}]$	244.32	330.45	366.48	571.14	
	$\tilde{\nu}_{C_1}/ \tilde{\nu}_{C_1} $	1.12	1.52	1.68	2.62	
	$b [\text{cm}^{-1}/\text{\AA}^2]$	649	1187	1460	3546	
	$a [\text{cm}^{-1}/\text{\AA}^4]$	2235	7478	11 312	66 730	
	$w_i [\%]$	2	54	14	22	
HDH $ \tilde{\nu}_{C_1}  = 204.2 \text{ cm}^{-1} \mu_{Cs} = 1.80$	$\tilde{\nu}_{C_1} [\text{cm}^{-1}]$	321.7	351.74	428.45		
	$\tilde{\nu}_{C_1}/ \tilde{\nu}_{C_1} $	1.58	1.72	2.10		
	$b [\text{cm}^{-1}/\text{\AA}^2]$	1382	1652	2451		
	$a [\text{cm}^{-1}/\text{\AA}^4]$	10 137	14 488	31 894		
	$w_i [\%]$	69	17	7		
DHH $ \tilde{\nu}_{C_1}  = 182.8 \text{ cm}^{-1} \mu_{Cs} = 2.62$	$\tilde{\nu}_{C_1} [\text{cm}^{-1}]$	215.55	242.48	270.97	545	563.87
	$\tilde{\nu}_{C_1}/ \tilde{\nu}_{C_1} $	1.18	1.33	1.47	2.95	3.08
	$b [\text{cm}^{-1}/\text{\AA}^2]$	901	1140	1424	5759	6165
	$a [\text{cm}^{-1}/\text{\AA}^4]$	4307	6898	10 757	176 040	201 717
	$w_i [\%]$	23	2	39	8	24
DDH $ \tilde{\nu}_{C_1}  = 175.6 \text{ cm}^{-1} \mu_{Cs} = 3.05$	$\tilde{\nu}_{C_1} [\text{cm}^{-1}]$	213.78	269.56	384.95	412.31	418.48
	$\tilde{\nu}_{C_1}/ \tilde{\nu}_{C_1} $	1.22	1.54	2.19	2.35	2.38
	$b [\text{cm}^{-1}/\text{\AA}^2]$	1032	1641	3346	3838	3954
	$a [\text{cm}^{-1}/\text{\AA}^4]$	5651	14 285	59 412	78 190	82 977
	$w_i [\%]$	28	41	6	9	15

**Table 4. Corrections to the Ground State ZPE Obtained in the Model Calculations<sup>a</sup>**

HHH	$1/2\tilde{\nu}_{C_1}$	122.16	165.23	183.24	285.57	
	ZPE <sub>model</sub>	68.15	94.48	106.64	186.20	
	ZPE <sub>model</sub> – $1/2\tilde{\nu}_{C_1}$	–54.01	–70.74	–76.60	–99.37	
	$w_i [\%]$	2	54	14	22	
	ZPE corr.		–78.12			
HDH	$1/2\tilde{\nu}_{C_1}$	160.85	175.87	214.23		
	ZPE <sub>model</sub>	91.63	101.59	129.12		
	ZPE <sub>model</sub> – $1/2\tilde{\nu}_{C_1}$	–69.22	–74.28	–85.11		
	$w_i [\%]$	69	17	7		
	ZPE corr.		–71.34			
DHH	$1/2\tilde{\nu}_{C_1}$	107.78	121.24	135.49	272.50	281.94
	ZPE <sub>model</sub>	60.32	67.64	75.86	175.15	183.10
	ZPE <sub>model</sub> – $1/2\tilde{\nu}_{C_1}$	–47.46	–53.60	–59.62	–97.35	–98.83
	$w_i [\%]$	23	2	39	8	24
	ZPE corr.			–69.53		
DDH	$1/2\tilde{\nu}_{C_1}$	106.89	134.78	192.48	206.16	209.24
	ZPE <sub>model</sub>	59.85	75.44	113.11	122.98	125.25
	ZPE <sub>model</sub> – $1/2\tilde{\nu}_{C_1}$	–47.04	–59.34	–79.37	–83.18	–83.99
	$w_i [\%]$	28	41	6	9	15
	ZPE corr.			–62.98		

<sup>a</sup>%inv denotes the PED-based content brutto of the inversion in a given normal mode.

Since we use experimental data as reference, the aug-cc-pVDZ basis set is our natural selection for further modeling. By offering the best reproduction of differences in experimental vibrational frequencies between the S<sub>0</sub> and S<sub>1</sub> states, its use should highlight the effects of improved treatment of the NH<sub>2</sub> inversion. For the same reason (superior agreement of  $\Delta(\text{exc-gr})$  with experiment), the nonplanar conformation of AA has been adopted for the ground state calculations.

## 6. MODEL CALCULATIONS AND DISCUSSION

As was envisaged in section 4, for the sake of consistency the energy barrier of 49.6 cm<sup>–1</sup>, coming directly from the CC2/

aug-cc-pVDZ calculations, has been taken to parametrize the model potential. The remaining issue is to select the ground state normal modes that contain contributions of the NH<sub>2</sub> inversion. This has been done using the potential energy distribution method, as implemented in Turbomole. The frequencies of the chosen normal modes and the contents brutto of the NH<sub>2</sub> vibration in each of them are listed in Table 3. For the sake of conciseness, Table 3 contains only the XXH deuteromers. The data for the XXD ones are very similar, and can be found in the Supporting Information.

Analysis of the frequencies and the frequency ratios of  $\tilde{\nu}_{C_1}/|\tilde{\nu}_{C_1}|$  shows that for each isotopomer the normal mode that has



Table 5. Calculated versus Experimental<sup>41</sup> Relative Shifts [in cm<sup>-1</sup>] of the 0–0 Bands for Different Isotopomers of AA<sup>a</sup>

	exp.	uncorrected	$\Delta$	single-mode corrected	$\Delta$	multimode corrected	$\Delta$
HHH	0	0	0	0	0	0	0
HHD	9.75	10.27	0.52	10.06	0.31	11.02	1.27
HDH	43.46	48.72	5.26	47.20	3.74	41.94	−1.52
HDD	53.03	59.03	5.99	57.29	4.26	52.30	−0.73
DHH	−6.92	6.77	13.69	−4.35	2.57	−1.82	5.10
DHD	2.80	17.06	14.26	5.60	2.80	8.72	5.92
DDH	37.51	57.40	19.89	45.99	8.48	42.26	4.75
DDD	46.96	67.69	20.73	55.96	9.00	52.22	5.26

<sup>a</sup> $\Delta$  stands for the errors between the calculated and the experimental values.

the dominating contribution from the inversion of the amino group also has the frequency that satisfies approximately the condition  $\tilde{\nu}_{C_1}/|\tilde{\nu}_{C_2}| = \sqrt{2}$  characteristic for the quartic-quadratic model potential. On the other hand, the remaining vibrations also contain sizable contributions of the NH<sub>2</sub> inversion. Therefore we have taken them into account in the quasi-multidimensional approach, even though for some of them the frequency ratios considerably deviate from  $\sqrt{2}$ . For comparison, we will later show the results obtained using both the single-mode and the quasi-multimode schemes. Having parametrized the model, we have carried out numerical calculations of the ground state vibrational frequencies in the double well potential using the Numerov method.<sup>40</sup> The results are collected in Table 4. Again, the data for the XXD isotopomers have been left out and are available in the supplement. One can easily observe that the calculated energies of the ground vibrational state exceed the energy barrier by at least 10 cm<sup>-1</sup>. For the normal modes that contain the largest contributions of the NH<sub>2</sub> inversion, the differences are higher than 25 cm<sup>-1</sup>. The corresponding wave functions have single maxima corresponding to the planar conformation of the AA molecule, qualitatively resembling the solutions for a hypothetical, single-well, barrierless potential (an example can be seen in section 7). It is related to the concept of dynamical planarization used in some cases of aromatic amines to rationalize the fact that most of the vibronic details in the optical spectra can be reproduced theoretically assuming the planar conformations.

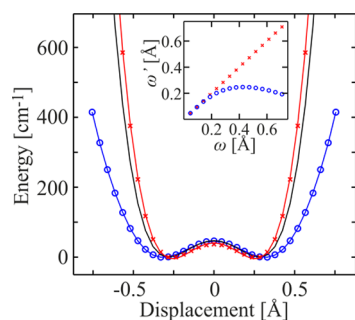
A closer look at the data presented in Table 4 shows that in all the cases, the numerically obtained values constitute approximately 60% of the respective frequencies from the harmonic vibrational analyses. Note, however, that the final ZPE corrections are not the same as the corrections for the normal modes that have the largest contents of the NH<sub>2</sub> inversion. These discrepancies vary from one isotopomer to another, owing to different distributions ( $w_i$ ) of the inversion among the ground-state normal modes. The relative shifts of the origin bands, calculated using the model corrections to the ground state ZPEs are collected in Table 5 and compared with the uncorrected shifts, based solely on the harmonic frequencies. The improvement brought about by the model corrections is evident. The corrected shifts are much closer to the experimental values. The relative shift of the HHD isotopomer has been virtually unaffected, which is consistent with our earlier observations that deuteration of the carboxylic group is practically decoupled from the effects of deuteration of the amino group. Moreover, the shift for the HHD species has been reproduced correctly already at the harmonic level, which shows that the errors are indeed related to the anharmonicity of the NH<sub>2</sub> large amplitude motions (inversion and torsion).

The multimode correction brings the shifts of the HDH and HDD isotopomers to almost perfect agreement with the experimental data. The shifts calculated for the remaining four isotopomers (DXY) are also improved, being now uniformly overshoot by  $\approx 5$  cm<sup>-1</sup>. Even though the overall agreement with experiment leaves some room for improvement, the model-corrected results are clearly superior to the uncorrected values, for which the errors exceed 20 cm<sup>-1</sup>. One can observe that the multimode corrected shifts are also somewhat better than the ones obtained using the simple, single-mode approach. The errors of the multimode results are more systematic and on average slightly smaller; nearly gone is the positive error of the shifts (on average  $\approx 6$  cm<sup>-1</sup>), observed in the single mode results for the XDX deuteromers. The agreement with experiment, however, remains imperfect—the shifts for DXX isotopomers are still overestimated by  $\approx 5$  cm<sup>-1</sup>, so the characteristic zigzag pattern of the uncorrected results is not entirely smoothed away. One of the possible causes of the errors is incorrect height of the energy barrier. The assumed value of 49 cm<sup>-1</sup>, coming directly from the CC2/aug-cc-pVDZ calculations, lies within the range of 40–55 cm<sup>-1</sup> based on the best available quantum chemistry calculations (see section 4). Nevertheless, we have checked that changing the energy barrier by  $\pm 10$  cm<sup>-1</sup> has little influence on the results. For details, the reader is referred to the Supporting Information.

Another potential source of the errors is the insufficient flexibility of the quartic-quadratic function used to represent the two-well potential for the NH<sub>2</sub> inversion. This function is the simplest model that captures the essential features of the two-well potential. Because of its simplicity it can be parametrized without laborious mapping of the PES. With only two terms of the Taylor expansion, however, while it reasonably well describes the PES in the vicinity and between the minima, it is bound to be less accurate for large displacements toward the umbrella conformations of the amino group. In order to verify this conjecture, we have performed a potential energy scan changing the dihedral angle  $\omega$  formed by the H–N–C plane (involving the free hydrogen atom of the amino group – denoted as site 1 in Figure 1) and the plane of the benzene ring, starting from the planar conformation of AA. The scan has been carried out in two ways:

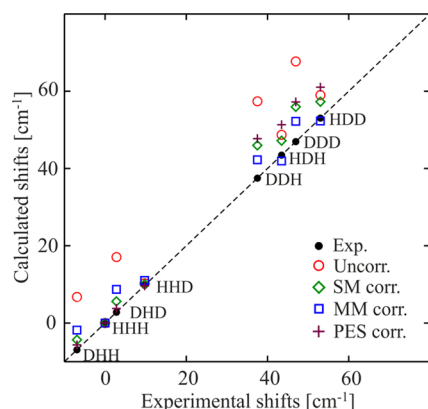
- the dihedral angle formed by the H–N–C plane involving the other amino hydrogen atom (site 2) with the plane of the benzene ring ( $\omega'$ ) kept equal to  $\omega$ ; the remaining degrees of freedom optimized at each point.
- the dihedral angle  $\omega'$  allowed to relax alongside the other molecular degrees of freedom.

Figure 5 shows the results of the scans together with the fitted polynomial curves, and with the model quartic-quadratic



**Figure 5.** Results of the potential energy scan for AA. Red x represents the symmetric scan ( $\omega' = \omega$ ), blue circles denote the energies of the relaxed scan ( $\omega'$  optimized). The inset shows the relation  $\omega'(\omega)$  during the scans. Black line with no symbols depicts the quartic-quadratic potential for the all H isotopomer (with parameters obtained using the frequency of  $330.45\text{ cm}^{-1}$ ).

potential for the all H isotopomer of AA. The resemblance of the potential that follows strictly the  $\text{NH}_2$  inversion ( $\omega' = \omega$ ) and the model curve is evident. The relaxed potential, on the other hand, is similar to the model only between the minima. Outside this region it is considerably less rigid. The reason for such a behavior can be seen in the inset, which shows the plot of  $\omega'(\omega)$ , represented as linear displacements of the hydrogen atoms.  $\omega'$  is approximately equal to  $\omega$  below  $0.25\text{ Å}$  ( $\approx 16$  degrees). For larger values of  $\omega$ , the other displacement remains below  $0.25\text{ Å}$ , and even decreases slightly for  $\omega > 0.43\text{ Å}$  ( $27$  degrees). Clearly, the  $\text{NH}_2$  inversion acquires admixtures of the torsional movement. The coupling of inversion and torsion can only be expected (the admixture of torsion can also be observed in the PED results for AA, as well as in the harmonic Cartesian displacements of the hydrogen atoms in the amino group (especially since the motion of the bridge hydrogen atom is somewhat limited, owing to the intramolecular hydrogen bond with the oxygen atom of the COOH group)). Thus obtained polynomial fit to the relaxed scan ( $\omega'$  unconstrained) has been subsequently used as the model potential energy with which the harmonic  $\text{ZPE}_{\text{gr}}$  was corrected (in the single mode approach) for all the deuteromers of AA. The results are presented in Figure 6 together with the uncorrected shifts and the results of the single mode and quasi-multimode calculations based on the quartic-quadratic potential



**Figure 6.** Calculated versus experimental relative shifts [in  $\text{cm}^{-1}$ ] of the 0–0 lines for different isotopomers of AA. SM, MM, and PES stand for single mode, multimode, and potential energy scan based approach, respectively (for details, see text).

function. The most striking feature of the new results is nearly complete reduction of the zigzag pattern characteristic for the results based on the quartic-quadratic model potentials. For the XHX deuteromers, the agreement is excellent. For the remaining four species, the calculated shifts show the uniform shift of  $8\text{--}10\text{ cm}^{-1}$ , but apart for that the trend and order of the 0–0 bands are correctly reproduced. One may thus conclude that the positive errors for the DXX isotopomers are caused by the quartic-quadratic potential being too steep in the regions corresponding to large deformations of the amino group.

On the other hand, the fact that the positive errors for the XDX isotopomers are observed in both single-mode approaches (that with the quartic-quadratic potential, and that based on the relaxed potential energy scan) reflects the need of at least two-dimensional model accounting for coupling of the torsion and inversion of the amino group. Nonetheless, for the extremely low-barrier case of AA even the simplest, single-mode quartic-quadratic model accounts for most of the errors introduced by using the standard vibrational analysis for the  $\text{NH}_2$  inversion. The semiquantitative agreement of the calculated shifts with the experimental data for one system can be viewed upon as fortuitous, although it may also indicate that systematic cancellation of errors takes place when the relative values of  $\Delta\text{ZPE}$  are calculated. In order to test our approach in more demanding cases of the intermediate inversion barrier, we have applied our models for three isomeric aminobenzonitriles.

## 7. AMINOBENZONITRILES: THE INTERMEDIATE BARRIER CASE

Aminobenzonitriles, or cyanoanilines (CA), are markedly different from AA: the  $\text{NH}_2$  inversion barrier is several times higher than for AA and the amino groups are not involved in the intramolecular hydrogen bonding. The ground state vibrational levels of the amino group inversion lie below the top of the barrier (for 3-CA and 3,5-dCA) or in close proximity of it (2-CA). Although tunneling through the barrier is still probable, the molecules cannot be regarded as dynamically planar (see Figure 7b), as it is in the case of AA (Figure 7a). The CAs represent thus the intermediate case, for which one can apply neither the perturbative approach based on the harmonic eigenfunctions of the barrierless potential, nor the harmonic solutions found locally for one of the two nearly isolated minima of the double-well potential. This is usually the most problematic situation for theoretical treatment, and we would like to use it to test the performance of our models. For this purpose we have selected o-cyanoaniline (2-CA), m-cyanoaniline (3-CA), and m,m-dicyanoaniline (3,5-dCA). Table 6 contains the energy barriers for the three compounds, the frequencies of the normal modes (for the nonplanar ground-state conformation), and the respective contributions of inversion of the amino group calculated for all of their deuteromers. As in the preceding section, all the results are based on the CC2/aug-cc-pVDZ calculations. The presented data show some interesting features. The energy barriers get lower in the following sequence: 3-CA > 3,5-dCA > 2-CA, which reflects the electron-withdrawing property of the CN groups. Its influence is considerably smaller for the *meta* positions in the benzene ring than for the *ortho* position. Therefore, the energy barrier for the 2-CA is even lower than for the doubly substituted 3,5-dCA. Moreover, the  $\pi$ -conjugated system of 2-CA favors the resonance structure in which the amino group acquires a partial positive charge, while

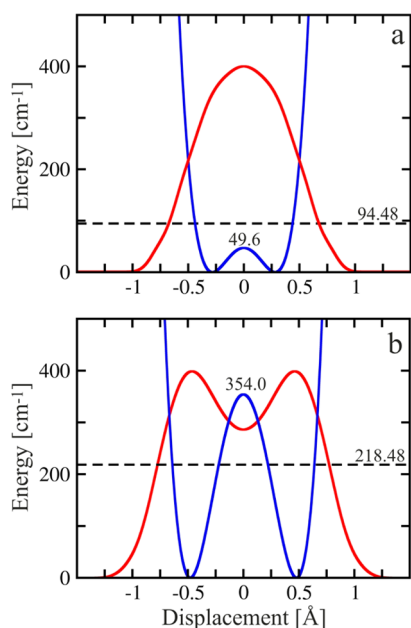


**Figure 7.** The model double-well potentials (blue lines), ZPE levels (dashed lines), and the corresponding vibrational wave functions (red lines) for the all H isotopomers of AA (upper panel) and 3-CA (lower panel).

the nitrogen atom of the CN group becomes partly negative. Small distance between the two groups leads to sizable electrostatic interactions between them. The hydrogen atom closer to the CN group is bound to be particularly affected. The inequivalence of the hydrogen atoms of the NH<sub>2</sub> group is reflected in increased differences between the frequencies of inversion (obtained for the planar ground-state conformation)

$|\tilde{\nu}_{\text{CS}}|$  and the reduced masses for the HD and DH deuteromers of 2-CA, as compared to the respective isotopomers of 3-CA.

The higher energy barriers for the cyanoanilines with respect to AA result in much higher frequencies of inversion, as calculated both for the planar and for the distorted ground state conformations (cf. tables 3 and 6). The model corrections, on the other hand, are relatively smaller than for the AA. It comes as no surprise, as they should disappear in the limit of the infinite energy barrier, for which the frequencies obtained for one of the local minima would be exact in the framework of the harmonic approximation. Table 7 contains the calculated shifts

**Table 7. Calculated and Experimental Relative Shifts (in cm<sup>-1</sup>) of the 0–0 Lines for Isotopomers of the Selected Cyanoanilines<sup>a</sup>**

		uncorrected	single mode corrected	quasi-multimode corrected	experimental
3-CA	HH	0.0	0.0	0.0	0
	HD	11.2	−3.4	−8.3	−7.5*
	DH	13.9	1.3	−3.4	−5.5*
	DD	27.4	−7.4	−7.3	−7.5
3,5-dCA	HH	0.0	0.0	0.0	0
	HD	11.8	−0.9	−4.5	−9.4
	DD	25.5	−10.8	−12.4	−15.9
2-CA	HH	0.0	0.0	0.0	0
	HD	20.6	−1.7	−5.2	−6*
	DH	14.5	−1.3	−14.0	−14.7*
	DD	36.3	−0.4	−17.2	−18.6

<sup>a</sup>The experimental values that have been assigned to particular deuteromers based on the theoretical results are marked with an asterisk.

**Table 6. Energy Barriers and Frequencies of the Selected Normal Modes, with the PED-Based Contributions of the NH<sub>2</sub> Inversion**

3-CA $\Delta_{\text{adZ}} = 354 \text{ cm}^{-1}$ $\Delta_{\text{CBS}}^a \approx 341 \text{ cm}^{-1}$	HH	$ \tilde{\nu}_{\text{CS}}  = 427.4 \text{ cm}^{-1}$ $\mu_{\text{CS}} = 1.28$	$\tilde{\nu}_{\text{C}} [\text{cm}^{-1}]$	523.2	569.9	619.0	640.4	
			%inv	0.02	0.52	0.24	0.12	
	HD	$ \tilde{\nu}_{\text{CS}}  = 381.2 \text{ cm}^{-1}$ $\mu_{\text{CS}} = 1.70$	$\tilde{\nu}_{\text{C}} [\text{cm}^{-1}]$	453.7	515.5	612.3		
			%inv	0.08	0.71	0.09		
	DH	$ \tilde{\nu}_{\text{CS}}  = 373.2 \text{ cm}^{-1}$ $\mu_{\text{CS}} = 1.81$	$\tilde{\nu}_{\text{C}} [\text{cm}^{-1}]$	451.7	519.0	523.1	547.3	610.2
			%inv	0.06	0.05	0.58	0.08	0.08
	DD	$ \tilde{\nu}_{\text{CS}}  = 332.6 \text{ cm}^{-1}$ $\mu_{\text{CS}} = 2.78$	$\tilde{\nu}_{\text{C}} [\text{cm}^{-1}]$	429.3	479.8	608.3		
			%inv	0.53	0.38	0.04		
3,5-dCA $\Delta_{\text{adZ}} = 249 \text{ cm}^{-1}$ $\Delta_{\text{CBS}}^a \approx 240 \text{ cm}^{-1}$	HH	$ \tilde{\nu}_{\text{CS}}  = 394.0 \text{ cm}^{-1}$ $\mu_{\text{CS}} = 1.28$	$\tilde{\nu}_{\text{C}} [\text{cm}^{-1}]$	519.8	550.9	606.1		
			%inv	0.55	0.25	0.13		
	HD	$ \tilde{\nu}_{\text{CS}}  = 346.9 \text{ cm}^{-1}$ $\mu_{\text{CS}} = 1.77$	$\tilde{\nu}_{\text{C}} [\text{cm}^{-1}]$	477.0	603.2			
			%inv	0.77	0.06			
	DD	$ \tilde{\nu}_{\text{CS}}  = 306.2 \text{ cm}^{-1}$ $\mu_{\text{CS}} = 2.77$	$\tilde{\nu}_{\text{C}} [\text{cm}^{-1}]$	394.9	428.3			
			%inv	0.45	0.46			
	HH	$ \tilde{\nu}_{\text{CS}}  = 364.8 \text{ cm}^{-1}$ $\mu_{\text{CS}} = 1.32$	$\tilde{\nu}_{\text{C}} [\text{cm}^{-1}]$	471.51	512.81			
			%inv	0.13	0.75			
2-CA $\Delta_{\text{adZ}} = 192 \text{ cm}^{-1}$ $\Delta_{\text{CBS}}^a \approx 182 \text{ cm}^{-1}$	HD	$ \tilde{\nu}_{\text{CS}}  = 326.2 \text{ cm}^{-1}$ $\mu_{\text{CS}} = 1.77$	$\tilde{\nu}_{\text{C}} [\text{cm}^{-1}]$	437.74	441.45	486.69		
			%inv	0.59	0.15	0.18		
	DH	$ \tilde{\nu}_{\text{CS}}  = 314.8 \text{ cm}^{-1}$ $\mu_{\text{CS}} = 1.97$	$\tilde{\nu}_{\text{C}} [\text{cm}^{-1}]$	204.47	272.54	445.5	457.11	492.3
			%inv	0.04	0.09	0.04	0.43	0.35
	DD	$ \tilde{\nu}_{\text{CS}}  = 284.4 \text{ cm}^{-1}$ $\mu_{\text{CS}} = 2.86$	$\tilde{\nu}_{\text{C}} [\text{cm}^{-1}]$	203.95	376.13	390.2	483.1	
			%inv	0.05	0.09	0.78	0.06	

<sup>a</sup> $\Delta_{\text{CBS}}$  for all cases was based on D,T extrapolation from the aug-cc-PVXZ results.

of the 0–0 lines for the deuteromers of the studied cyanoanilines. One can easily see, that the shifts are considerably smaller than for AA, as no internal hydrogen bond is present here. They are neither so regular nor additive, because, unlike in the case of AA, the hydrogen atoms are strongly coupled within the amino group, and substituting one of the atoms with deuterium affects the motions of both of them.

Apart from the theoretical work, we also measured the LIF excitation spectra for all three cyanoanilines seeded in the supersonic jet, with three levels of deuteration (0%, ~50%, and ~90%). The experimental setup and methodology of recording of the spectra were described in our previous work.<sup>12</sup> Figure 8

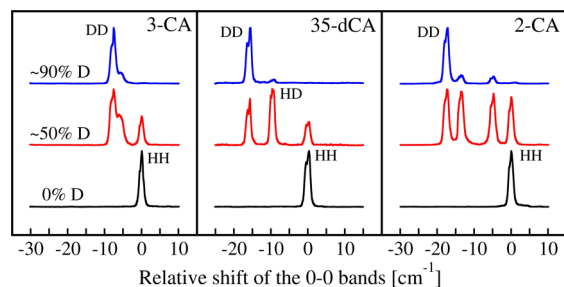


**Figure 8.** Experimental spectra (energy regions of the 0–0 bands) of three isomeric cyanoanilines with different levels of the isotopic exchange, showing deuteriation-induced shifts and partial assignment based on the relative intensities of the bands.

shows the energy region of the 0–0 transition, in which the origin bands of the excitation spectra are visible. The relative intensities of the bands for different deuteromers allowed for unambiguous identification of the HH and DD isotopomers, and in the case of the symmetric 3,5-dCA, also of the HD isotopomer. The singly substituted deuteromers of the asymmetric cyanoanilines could not be identified without additional data. Comparison of the experimentally determined and theoretically calculated shifts of the 0–0 bands (table 7 and Figure 9) shows that the uncorrected results are qualitatively wrong, predicting blue shift due to deuteration instead of the observed red shift.

The single-mode model corrections have brought the theoretical results somewhat closer to the experimental values, but unlike the case of AA, for most of the cyanoaniline deuteromers the corrections have been insufficient to reach even qualitative agreement with experiment. Only for the DD isotopomers of 3-CA and 3,5-dCA do the calculated shifts approached the measured ones. Clearly, for systems characterized by higher inversion barriers than AA, the assumption of one-dimensionality of the potential is more difficult to satisfy. Such systems are more distorted from planarity at the bottom of the potential well: the angles between the CN bond and the NHH plane, as calculated at the CC2/aug-cc-pVDZ level of theory are 42.4, 39.5, and 37.4 degrees for 3-CA, 3,5-dCA, and 2-CA, respectively, whereas for AA the angle is 28.4 degrees. Consequently, the mixing of the  $\text{NH}_2$  inversion mode with other normal modes is stronger, and so is the need to include it in the model calculations. Hence the better performance of the quasi-multimode approach, which has been able to bring the shifts for all of the cyanoaniline deuteromers to at least semiquantitative agreement with experiment. The agreement is particularly good for 2-CA, for which the calculated shift for the DD isotopomer matches the experimental value within the

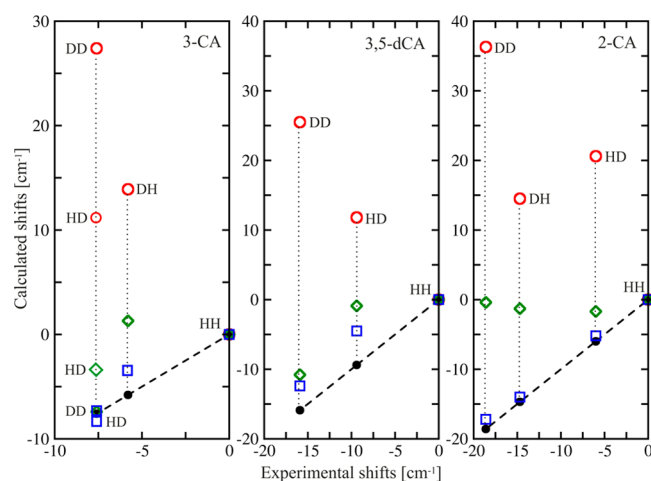


**Figure 9.** Experimental (black bullets) versus calculated relative positions of the 0–0 lines for deuteromers of the studied cyanoanilines. Red circles (○) denote the noncorrected results, green diamonds (◇) represent the results corrected with the simpler, single-mode model, and blue squares (□) stand for the results corrected in the multimode approach.

margin of  $1.5 \text{ cm}^{-1}$ . The calculated shifts for the singly substituted deuteromers (HD and DH) of 2-CA are also in agreement with the two remaining experimental values. Based on our results, we could assign the band at  $\sim 6 \text{ cm}^{-1}$  in the spectrum of 2-CA to the HD isotopomer, and the band at  $\sim 14.7 \text{ cm}^{-1}$  to the DH one. In the case of 3-CA, the origin bands for deuterated species partly overlap one another as the differences between the shifts are less than the width of individual bands. The intensity analysis shows, however, that the shoulder on the high energy side of the band at  $7.5 \text{ cm}^{-1}$  is due to absorption of one of the asymmetrically deuterated species (HD or DH). The 0–0 bands of the remaining two deuteromers are localized at the same (within the resolution limit) energy, which is reflected in the nearly doubled intensity of the band at  $7.5 \text{ cm}^{-1}$  with respect to that of the HH isotopomer (and also of the shoulder at  $5.5 \text{ cm}^{-1}$ ) observed in the spectrum of a sample with  $\sim 50\%$  of the isotopic exchange.

The calculated shift for the DD isotopomer of 3-CA is again in excellent agreement with the experimental one. The values for the asymmetrically deuterated species corroborate the conclusions of the analysis based on the observed band intensities: the band of the DH isotopomer is predicted to be shifted less by  $3.9 \text{ cm}^{-1}$  than the band of the DD isotopomer, which, in turn, nearly coincides energetically with the band of the HD species. These results reflect the already discussed inequivalence of the two hydrogen atoms of the amino group in the asymmetrically substituted cyanoanilines. The conclusions derived from our model calculations for 3-CA, however, have to be treated with more caution, owing to small values of the shifts that are comparable with errors of the model calculations for other systems studied in this work. Conclusive predictions in this case require more elaborate (truly multidimensional) theoretical models and, possibly, higher resolution experimental spectra.

## 8. CONCLUSIONS

At the examples of AA and three cyanoanilines, we have shown that the standard vibrational analyses based on the harmonic approximation leads to qualitatively incorrect results concern-



ing the deuteration induced shifts of the electronic origins of the absorption spectra. In order to correct the theoretical results, the frequency of the  $\text{NH}_2$  inversion from the harmonic calculations has been replaced by the frequency obtained using a one-dimensional quartic-quadratic model potential, the parameters of which are derived from the harmonic frequency and the energy barrier for the inversion. This correction has brought about a considerable improvement of the calculated shifts of the 0–0 bands for the AA deuteromers. The deviations from the experimental values, however, have not been completely removed: the relative shifts (with respect to the all H isotopomer) for the XDX deuteromers are systematically overestimated, as are the shifts for the DXX species. In order to improve the accuracy, a quasi-multimode approach has been proposed, in which the model corrections are introduced individually to all the normal modes mixed with the  $\text{NH}_2$  inversion. This modification has reduced the systematic error for the XDX deuteromers, leaving only the uniform positive error of  $5\text{ cm}^{-1}$  for the DXX species. The single mode scheme with a potential based on the relaxed potential energy scan rather than on the quartic-quadratic function has removed the error for the DXX deuteromers, but for the XDX ones the uniform ( $\approx 9\text{ cm}^{-1}$ ) overestimation of the shifts can still be observed. The errors for the XDX deuteromers can thus be associated with one-dimensionality of the model, whereas the deviations from experimental values for the DXX deuteromers are related to the character of the quartic-quadratic function itself, which rises too steeply for large displacements of the amino group from planarity. On the other hand, the harmonic approximation used for all the remaining normal modes has little impact on the relative shifts of the 0–0 bands of deuteromers of AA. In view of the above observations, one may expect to achieve an excellent agreement with experiment by using a two-dimensional model accounting simultaneously for the inversion and torsion of the amino group and, possibly, a more realistic model of the inversion potential. Nevertheless, even the simple approach described above leads to over 3-fold reduction of errors for AA, and for cyanoanilines the qualitatively wrong uncorrected results (reversed trends with respect to experiment) have been brought to at least semiquantitative agreement with the experimental values, which allowed for identification of the unassigned 0–0 bands for deuteromers of 2-CA and 3-CA. Therefore, owing to its simplicity and relatively low computational cost (the laborious potential energy mapping is entirely avoided), we recommend the presented approach as the first step toward estimating the deuteration-induced shifts of the electronic origins in the optical spectra of aromatic amines. It should be especially worthwhile if differences between the 0–0 band energies for different deuteromers exceed  $5\text{ cm}^{-1}$ . Otherwise conclusive assignment may require the more accurate, fully multidimensional approach.

## ■ ASSOCIATED CONTENT

### ■ Supporting Information

Full version of Table 3 (Table S1) containing information also for the XXD isotopomers of AA; Table S2 and Figure S1 showing results of the model calculations for different values of energy barrier for the AA. This material is available free of charge via the Internet at <http://pubs.acs.org>

## ■ AUTHOR INFORMATION

### Corresponding Author

\*Phone: +48 12 6632023; e-mail: [andrzej@chemia.uj.edu.pl](mailto:andrzej@chemia.uj.edu.pl).

### Notes

The authors declare no competing financial interest.

## ■ ACKNOWLEDGMENTS

This research was carried out in part with the equipment purchased thanks to the financial support of the European Regional Development Fund in the framework of the Polish Innovation Economy Operational Program (contract no. POIG.02.01.00-12-023/08). This research was also supported in part by PL-Grid Infrastructure, with the calculations performed on Zeus: HP Cluster Platform of the Academic Computer Centre CYFRONET.

## ■ REFERENCES

- (1) Yu, H.; Joslin, E.; Crystall, B.; Smith, T.; Sinclair, W.; Philips, D. Spectroscopy and Dynamics of Jet-Cooled 4-Aminobenzonitrile (4-ABN). *J. Phys. Chem.* **1993**, *97*, 8146–8151.
- (2) Zierkiewicz, W.; Komorowski, L.; Michalska, D.; Cerny, J.; Hobza, P. The Amino Group in Adenine: MP2 and CCSD(T) Complete Basis Set Limit Calculations of the Planarization Barrier and DFT/B3LYP Study of the Anharmonic Frequencies of Adenine. *J. Phys. Chem. B* **2008**, *112*, 16734–16740.
- (3) Wojciechowski, P. M.; Zierkiewicz, W.; Michalska, D.; Hobza, P. Electronic structures, vibrational spectra, and revised assignment of aniline and its radical cation: Theoretical study. *J. Chem. Phys.* **2003**, *118*, 10900–10911.
- (4) Kolek, P.; Pirowska, K.; Chacaga, Ł.; Najbar, J. LIF excitation spectra of jet-cooled 3,5-dicyanoaniline. *Phys. Chem. Chem. Phys.* **2003**, *5*, 4096–4107.
- (5) Kolek, P.; Pirowska, K.; Najbar, J. LIF excitation spectra of o- and m-cyanoanilines. *Phys. Chem. Chem. Phys.* **2001**, *3*, 4874–4888.
- (6) Berden, G.; Meerts, W. L.; Plusquellic, D. F.; Fujita, I.; Pratt, D. W. High resolution electronic spectroscopy of 1-aminonaphthalene:  $S_0$  and  $S_1$  geometries and  $S_1 \rightarrow S_0$  transition moment orientations. *J. Chem. Phys.* **1996**, *104*, 3935–3946.
- (7) Wang, S.; Schaefer, H. S. The small planarization barriers for the amino group in the nucleic acid bases. *J. Chem. Phys.* **2006**, *124*, 044303(1–8).
- (8) Pirowska, K.; Kolek, P.; Goclon, J.; Najbar, J. Geometry changes upon  $S_0 \rightarrow S_1$  electronic excitation of aniline derivatives. *Chem. Phys. Lett.* **2004**, *387*, 165–175.
- (9) Bludský, O.; Šponer, J.; Leszczynski, J.; Špirko, V.; Hobza, P. Amino groups in nucleic acid bases, aniline, aminopyridines and aminotriazine are nonplanar: results of correlated ab initio quantum chemical calculations and anharmonic analysis of the aniline inversion motion. *J. Chem. Phys.* **1996**, *105*, 11042–11050.
- (10) Leśniewski, S.; Kolek, P.; Pirowska, K.; Sobolewski, A. L.; Najbar, J. Franck-Condon analysis of laser-induced fluorescence excitation spectrum of anthranilic acid: Evaluation of geometry change upon  $S_0 \rightarrow S_1$  excitation. *J. Chem. Phys.* **2009**, *130*, 054307(1–14).
- (11) Andrzejak, M.; Pawlikowski, M. T. Vibronic Effects in the  $1^1B_u(1^1B_2)$  Excited Singlet States of Oligothiophenes. Fluorescence Study of the  $1^1A_g(1^1A_1) \rightarrow 1^1B_u(1^1B_2)$  transition in Terms of DFT, TDDFT, and CASSCF Methods. *J. Phys. Chem. A* **2008**, *112*, 13737–13744.
- (12) Kolek, P.; Leśniewski, S.; Andrzejak, M.; Góra, M.; Cias, P.; Węgrzynowicz, A.; Najbar, J. LIF excitation spectra for  $S_0 \rightarrow S_1$  transition of deuterated anthranilic acid (COOD, ND2) in supersonic-jet expansion. *J. Mol. Spectrosc.* **2010**, *264*, 129–136.
- (13) Pyka, J.; Kreglewski, M. Vibration-inversion-torsion-rotation Hamiltonian for aniline. *J. Mol. Spectrosc.* **1985**, *109*, 207–220.

- (14) Kwiatkowski, J. S.; Leszczynski, J. Molecular structure and vibrational IR spectrum of formamide revisited: ab initio post-Hartree-Fock study. *J. Mol. Struct.* **1993**, 297, 277–284.
- (15) McCarthy, W. J.; Lapinski, L.; Nowak, M. J.; Adamowicz, L. Anharmonic contributions to the inversion vibration in 2-aminopyrimidine. *J. Chem. Phys.* **1995**, 103, 656–662.
- (16) Becke, A. D. A new mixing of Hartree-Fock and local density-functional theories. *J. Chem. Phys.* **1993**, 98, 1372–1377.
- (17) Lee, C.; Yang, W.; Parr, R. G. Development of the Colle-Salvetti correlation-energy formula into a functional of the electron density. *Phys. Rev. B* **1988**, 37, 785–789.
- (18) Vosko, S. H.; Wilk, L.; Nusair, M. Accurate spin-dependent electron liquid correlation energies for local spin density calculations: A critical analysis. *Can. J. Phys.* **1980**, 58, 1200–1211.
- (19) Adamo, C.; Barone, V. Toward reliable density functional methods without adjustable parameters: The PBE0 model. *J. Chem. Phys.* **1999**, 110, 6158–6169.
- (20) Christiansen, O.; Koch, H.; Jørgensen, P. The second-order approximate coupled cluster singles and doubles model CC2. *Chem. Phys. Lett.* **1995**, 243, 409–418.
- (21) Koch, H.; Christiansen, O.; Jørgensen, P.; Olsen, J. Excitation energies of BH, CH<sub>2</sub> and Ne in full configuration interaction and the hierarchy CCS, CC2, CCSD and CC3 of coupled cluster models. *Chem. Phys. Lett.* **1995**, 244, 75–82.
- (22) Hättig, C. Geometry optimizations with the coupled-cluster model CC2 using the resolution-of-the-identity approximation. *J. Chem. Phys.* **2003**, 118, 7751–7761.
- (23) Köhn, A.; Hättig, C. Analytic gradients for excited states in the coupled-cluster model CC2 employing the resolution-of-the-identity approximation. *J. Chem. Phys.* **2003**, 119, 5021–5036.
- (24) Schreiber, M.; Silva-Junior, M. R.; Sauer, S. P. A.; Thiel, W. Benchmarks for electronically excited states: CASPT2, CC2, CCSD, and CC3. *J. Chem. Phys.* **2008**, 128, 134110(1–25).
- (25) TURBOMOLE V6.3 2011, a development of University of Karlsruhe and Forschungszentrum Karlsruhe GmbH, 1989–2007, TURBOMOLE GmbH, since 2007; <http://www.turbomole.com>.
- (26) Klopper, W.; Samson, C. C. M. Explicitly correlated second-order Møller–Plesset methods with auxiliary basis sets. *J. Chem. Phys.* **2002**, 116, 6397–6410.
- (27) Tew, D. P.; Klopper, W.; Neiss, C.; Hättig, C. Quintuple-dzeta quality coupled-cluster correlation energies with triple- $\zeta$  basis sets. *Phys. Chem. Chem. Phys.* **2007**, 9, 1921–1930.
- (28) Köhn, A.; Richings, G. W.; Tew, D. P. Implementation of the full explicitly correlated coupled-cluster singles and doubles model ccscf12 with optimally reduced auxiliary basis dependence. *J. Chem. Phys.* **2008**, 129, 201103.
- (29) Hollas, J. M. *High resolution spectroscopy*; Butterworth: London, 1982.
- (30) Chan, S. I.; Zinn, J.; Fernandez, J.; Gwinn, W. D. Trimethylene Oxide. I. Microwave Spectrum, Dipole Moment, and Double Minimum Vibration. *J. Chem. Phys.* **1960**, 33, 1643.
- (31) Coon, J. B.; Naugle, N. W.; McKenzie, R. D. The investigation of double-minimum potentials in molecules. *J. Mol. Spectrosc.* **1966**, 20, 107–129.
- (32) Dunning, T. H. J. Gaussian basis sets for use in correlated molecular calculations. I. The atoms boron through neon and hydrogen. *J. Chem. Phys.* **1989**, 90, 1007–1023.
- (33) Halkier, A.; Helgaker, T.; Jørgensen, P.; Klopper, W.; Koch, H.; Olsen, J.; Wilson, A. K. Basis-set convergence in correlated calculations on Ne, N<sub>2</sub>, and H<sub>2</sub>O. *Chem. Phys. Lett.* **1998**, 286, 243–252.
- (34) Kolek, P.; Leśniewski, S.; Pirowska, K.; Najbar, J. LIF excitation spectra for S<sub>0</sub>→S<sub>1</sub> transition of anthranilic acid: Detailed studies. *J. Mol. Spectrosc.* **2008**, 249, 100–112.
- (35) Southern, C. A.; Levy, D. H.; Florio, G. M.; Longarte, A.; Zwier, T. S. Electronic and Infrared Spectroscopy of Anthranilic Acid in a Supersonic Jet. *J. Chem. Phys.* **2003**, 117, 4032–4040.
- (36) NIST Mass Spec Data Center, S. E. Stein, director. "Infrared Spectra" in *NIST Chemistry WebBook, NIST Standard Reference Database Number 69*; Linstrom, P. J., Mallard, W. G., Eds.; National Institute of Standards and Technology, Gaithersburg MD, 20899, <http://webbook.nist.gov> (Accessed Oct. 11, 2012).
- (37) Stearns, J. A.; Das, A.; Zwier, T. S. Hydrogen atom dislocation in the excited state of anthranilic acid: probing the carbonyl stretch fundamental and the effects of water complexation. *Phys. Chem. Chem. Phys.* **2004**, 6, 2605–2610.
- (38) Helgaker, T.; Gauss, J.; Jørgensen, P.; Olsen, J. The prediction of molecular equilibrium structures by the standard electronic wavefunctions. *J. Chem. Phys.* **1997**, 106, 6430–6440.
- (39) Coriani, S.; Marchesan, D.; Gauss, J.; Hättig, C.; Helgaker, T.; Jørgensen, P. The accuracy of ab initio molecular geometries for systems containing second-row atoms. *J. Chem. Phys.* **2005**, 123, 184107(1–12).
- (40) Numerov, B. V. Note on the numerical integration of  $d^2x/dt^2 = f(x,t)$ . *Astron. Nachr.* **1927**, 230, 359–364.
- (41) Kolek, P.; Andrzejak, M.; Najbar, J. Isotopic effects in the S<sub>1</sub> excited state of anthranilic acid deuterated in various positions. Supersonic-jet LIF spectroscopy and CC2 ab initio study. *J. Mol. Spectrosc.*, to be submitted for publication.